PLOS | ONE

RESEARCH ARTICLE

L17A/F19A Substitutions Augment the α-Helicity of β-Amyloid Peptide Discordant Segment

Chu-Ting Liang[1,2☯], Hsien-Bin Huang[3☯], Chih-Ching Wang[4,5], Yi-Ru Chen[4,6], Chi-Fon Chang[7], Ming-Shi Shiao[8], Yi-Cheng Chen[9]*, Ta-Hsien Lin[1,2,4,5]*

1 Department of Life Sciences and Institute of Genome Sciences, National Yang-Ming University, Taipei, Taiwan, R.O.C, **2** Basic Research Division, Medical Research Department, Taipei Veterans General Hospital, Taipei, Taiwan, R.O.C, **3** Department of Life Science and the Institute of Molecular Biology, National Chung Cheng University, Chiayi, Taiwan, R.O.C, **4** Structural Biology Program, National Yang-Ming University, Taipei, Taiwan, R.O.C, **5** Institute of Biochemistry & Molecular Biology, National Yang-Ming University, Taipei, Taiwan, R.O.C, **6** Department and Institute of Pharmacology, National Yang-Ming University, Taipei, Taiwan, R.O.C, **7** Genomics Research Center, Academia Sinica, Taipei, Taiwan, R.O.C, **8** Department of Biomedical Sciences, Chang Gung University, Taoyuan, Taiwan, R.O.C, **9** Department of Medicine, Mackay Medical College, Taipei, Taiwan, R.O.C

☯ These authors contributed equally to this work.
* chen15@mmc.edu.tw (YCC); thlin@vghtpe.gov.tw (THL)

Citation: Liang C-T, Huang H-B, Wang C-C, Chen Y-R, Chang C-F, Shiao M-S, et al. (2016) L17A/F19A Substitutions Augment the α-Helicity of β-Amyloid Peptide Discordant Segment. PLoS ONE 11(4): e0154327. doi:10.1371/journal.pone.0154327

Editor: Eugene A. Permyakov, Russian Academy of Sciences, Institute for Biological Instrumentation, RUSSIAN FEDERATION

Received: January 14, 2016

Accepted: April 12, 2016

Published: April 22, 2016

Data Availability Statement: All relevant data are within the paper.

Funding: This work was supported by grants from the National Science Council of the Republic of China (NSC99-2320-B-194-003-MY3, NSC101-2113-M-010-003-MY2 and MOST103-2113-M-010-002), Taipei Veterans General Hospital, Taiwan, ROC (V100C-180, V101C-003 and V102C-037) and a grant from Ministry of Education, Aiming for the Top University Plan.

Abstract

β-amyloid peptide (Aβ) aggregation has been thought to be associated with the pathogenesis of Alzheimer's disease. Recently, we showed that L17A/F19A substitutions may increase the structural stability of wild-type and Arctic-type $A\beta_{40}$ and decrease the rates of structural conversion and fibril formation. However, the underlying mechanism for the increase of structural stability as a result of the alanine substitutions remained elusive. In this study, we apply nuclear magnetic resonance and circular dichroism spectroscopies to characterize the $A\beta_{40}$ structure, demonstrating that L17A/F19A substitutions can augment the α-helicity of the residues located in the α/β-discordant segment (resides 15 to 23) of both wild-type and Arctic-type $A\beta_{40}$. These results provide a structural basis to link the α-helicity of the α/β-discordant segment with the conformational conversion propensity of Aβ.

Introduction

β-amyloid peptide (Aβ), consisting of 39–42 residues, is derived from the proteolytic product of a type I transmembrane glycoprotein called β-amyloid precursor protein (AβPP). Alzheimer's disease (AD) is highly associated with Aβ aggregation. The molecular mechanism for Aβ aggregation remained unclear. The conformational change is occurred during the Aβ aggregation process. Recently, we have applied small Aβ-binding molecules to probe the aggregation mechanism of $A\beta_{40}$. The results indicated that the small molecules targeted to interact with the hydrophobic central region ($L_{17}VFFA_{21}$) of wild-type $A\beta_{40}$ can stabilize its conformation and block the formation of amyloid fibril [1]. Our previous structural characterizations by using

Competing Interests: The authors have declared that no competing interests exist.

Abbreviations: Aβ, β-amyloid peptide; AβPP, β-amyloid precursor protein; AD, Alzheimer's disease; CD, circular dichroism; CSI, chemical shift index; FAD, familial Alzheimer's disease; NMR, nuclear magnetic resonance; SDS, sodium dodecyl sulfate; TFE, trifluoroethanol.

nuclear magnetic resonance (NMR) spectroscopy, equilibrium denaturation and site-directed mutagenesis have also demonstrated that the secondary structure of the hydrophobic central region of Aβ was more prone to unfold than that of the rest of the regions in Aβ. Double replacements of the two residues (L17/F19) in this region by Alanine could block conformational changes and reduce cytotoxicity of wild-type $A\beta_{40}$ [2]. Arctic-type $A\beta_{40}$ ($A\beta_{40}$(E22G)), causing one of the familial Alzheimer's diseases (FAD), has been known to show a stronger aggregative ability than wild-type $A\beta_{40}$. By introducing double replacements (L17A/F19A) into Arctic-type $A\beta_{40}$, similar effects were also observed for this FAD-linked $A\beta_{40}$ variant [3], suggesting that the conformational stability in the hydrophobic central region of Aβ plays a critical role in the conformational conversion tendency of Aβ. There were also many studies of the hydrophobic central region of Aβ, which supported the view that the hydrophobic central region is highly correlated with Aβ aggregation and can be utilized for designing inhibitors [4–11].

The molecular mechanism for L17A/F19A substitutions to stabilize the conformations of the Aβ peptides remained unknown. By using circular dichroism (CD) spectroscopy, Johannson and coworkers showed that the overall α-helical propensity of $A\beta_{12-28}$ was increased after V18A/F19A/F20A replacements. This triple Ala-substituted $A\beta_{12-28}$ was predicted to form an α-helix in the region of the α/β-discordant segment, suggesting that V18A/F19A/F20A replacements abolished the discordance, resulting in inhibition of fibril formation of $A\beta_{12-28}$ [12]. It is likely that double replacements (L17A/F19A) could enhance the α-helicity in this region, in turn leading to an increase of their structural stability. However, it lacks the structural evidence to support this inference.

To demonstrate this hypothetic mechanism, we characterized the effects of L17A/F19A substitutions on the structures of wild-type and Arctic-type $A\beta_{40}$ by using nuclear magnetic resonance (NMR) and CD spectroscopies. Stable isotope labeled $A\beta_{40}$, $A\beta_{40}$(E22G), $A\beta_{40}$(L17A/F19A) and $A\beta_{40}$(L17A/F19A/E22G) were prepared in this study for NMR structural characterization. The propensity of secondary structure in these peptides were characterized in a residue-specific manner. An augmentation of α-helicity in the α/β-discordant segment was observed for both wild-type and Arctic-type $A\beta_{40}$ after L17A/F19A substitutions. These results may explain the reason why L17A/F19A substitutions increase the conformational stability of these two $A\beta_{40}$ peptides.

Materials and Methods

Sample Preparation

All Aβ peptides used in this study were produced using the protocols as described previously [13]. The cDNA of wild-type $A\beta_{40}$ was served as a template for the site-directed mutagenesis to create the cDNA of $A\beta_{40}$ mutants. All procedures followed the methods as described by manufacturer (QuikChange Lightning, Stratagene). Preparation of the stable isotope-labeled ($^{13}C/^{15}N$ and ^{15}N) Aβ peptides followed the methods as described in [2, 14].

CD Spectroscopy

All purified Aβ peptides that have been verified by mass spectrometry were pretreated with 100% TFE (trifluoroethanol) and then dried by nitrogen gas. The dried Aβ molecule was dissolved in 10 mM K_2HPO_4/KH_2PO_4 buffer solution containing 100 mM SDS-d_{25} (sodium dodecyl sulfate-d_{25}) (pH 6.0). All Aβ molecules (50 μM) were used for analysis by CD spectroscopy (Aviv410 spectropolarimeter, Aviv Biomedical, Inc., Lakewood, NJ USA). The spectra were collected at 296 K and the wavelengths were scanned from 190 to 260 nm in 0.2-nm

increments. The measurement was carried out three times. The secondary structure contents of Aβ were estimated by using CDNN program [15, 16].

NMR Spectroscopy

For NMR studies, the dried Aβ molecule was dissolved in 10 mM K_2HPO_4/KH_2PO_4 buffer solution containing 100 mM SDS-d_{25}, 10% (v/v) D_2O/H_2O, 0.02% NaN_3 and the internal chemical shift standard, TSP (3-(trimethylsilyl)propionic-2,2,3,3,-d_4 acid) (pH 6.0). The NMR data processing and the determination of backbone chemical shifts followed the methods as described in [2, 14].

Results

We first characterized the effect of L17A/F19A substitutions on the secondary structure contents of wild-type and Arctic-type $Aβ_{40}$ by using CD spectroscopy. The CD spectra of wild-type $Aβ_{40}$ and $Aβ_{40}$(L17A/F19A) in SDS solution were shown in Fig 1A. Both peptides exhibited two major bands in their CD spectra with minima at 206 and 220 nm (negative ellipticities at 206 and 220 nm). This spectral pattern is an indicative of α-helical structure for both peptides. In addition, the intensities at 206 and 220 nm were more negative for $Aβ_{40}$(L17A/F19A) than for wild-type $Aβ_{40}$, indicating that the α-helicity of $Aβ_{40}$(L17A/F19A) is higher than that of wild-type $Aβ_{40}$. The effect of L17A/F19A substitutions on the CD spectrum of Arctic-type $Aβ_{40}$ in SDS solution was shown in Fig 1B. The spectral patterns shown in Fig 1B were similar to those in Fig 1A. The intensities at 206 and 220 nm were a little bit more negative for $Aβ_{40}$(L17A/F19A/E22G) than for $Aβ_{40}$(E22G), suggesting that the conformation of $Aβ_{40}$(L17A/F19A/E22G) contains higher α-helicity than that of $Aβ_{40}$(E22G). We also used the CDNN program [15, 16] to analyze the CD spectra to estimate the secondary structure contents of wild-type $Aβ_{40}$, $Aβ_{40}$(L17A/F19A), $Aβ_{40}$(E22G) and $Aβ_{40}$(L17A/F19A/E22G). The results were shown in Table 1. Both double Ala-substituted Aβ peptides displayed higher α-helix and lower β-strand contents than their native forms. These findings indicated that double replacements (L17A/F19A) increased the α-helicity of both wild-type and Arctic-type $Aβ_{40}$. Since CD spectra can only provide information of overall structural differences, the region of these double Ala-substituted peptides for the increases of α-helical contents remained characterized.

We next applied NMR spectroscopy to analyze the structural differences between the double Ala-substituted Aβ peptides and their native forms. Fig 2A showed the 2D ^1H-^{15}N-HSQC spectrum of ^{15}N-labeled $Aβ_{40}$(L17A/F19A) in SDS solution. The assigned residues were indicated in the figure. The effect of L17A/F19A substitutions on the 2D ^1H-^{15}N-HSQC spectrum of wild-type $Aβ_{40}$ was shown in Fig 2B. It is apparent that some amide proton and nitrogen cross-peaks of wild-type $Aβ_{40}$ displayed noticeable chemical shift changes after the replacements of L17 and F19 with alanines. Compared to the previously assigned backbone resonances of wild-type $Aβ_{40}$ [14], these cross-peaks were identified as E11, H13-K16, V18, F20, E22, D23 and G25 (excluding L17 and F19). Fig 2C showed the backbone amide chemical shift differences between wild-type $Aβ_{40}$ and $Aβ_{40}$(L17A/F19A). Most of these residues that showed noticeable chemical shift changes after L17A/F19A substitutions were located within the α/β-discordant segment of wild-type $Aβ_{40}$. Fig 3A and 3B showed the 2D ^1H-^{15}N-HSQC spectrum of ^{15}N-labeled $Aβ_{40}$(L17A/F19A/E22G) without and with superimposition of the 2D ^1H-^{15}N-HSQC spectrum of ^{15}N-labeled $Aβ_{40}$(E22G), respectively. Comparison of the 2D ^1H-^{15}N-HSQC spectra for $Aβ_{40}$(E22G) and $Aβ_{40}$(L17A/F19A/E22G) in Fig 3B showed that noticeable chemical shift changes also occurred on some amide proton and nitrogen cross-peaks of $Aβ_{40}$(E22G) after L17A/F19A substitutions. Cross-peaks that displayed noticeable chemical shift changes

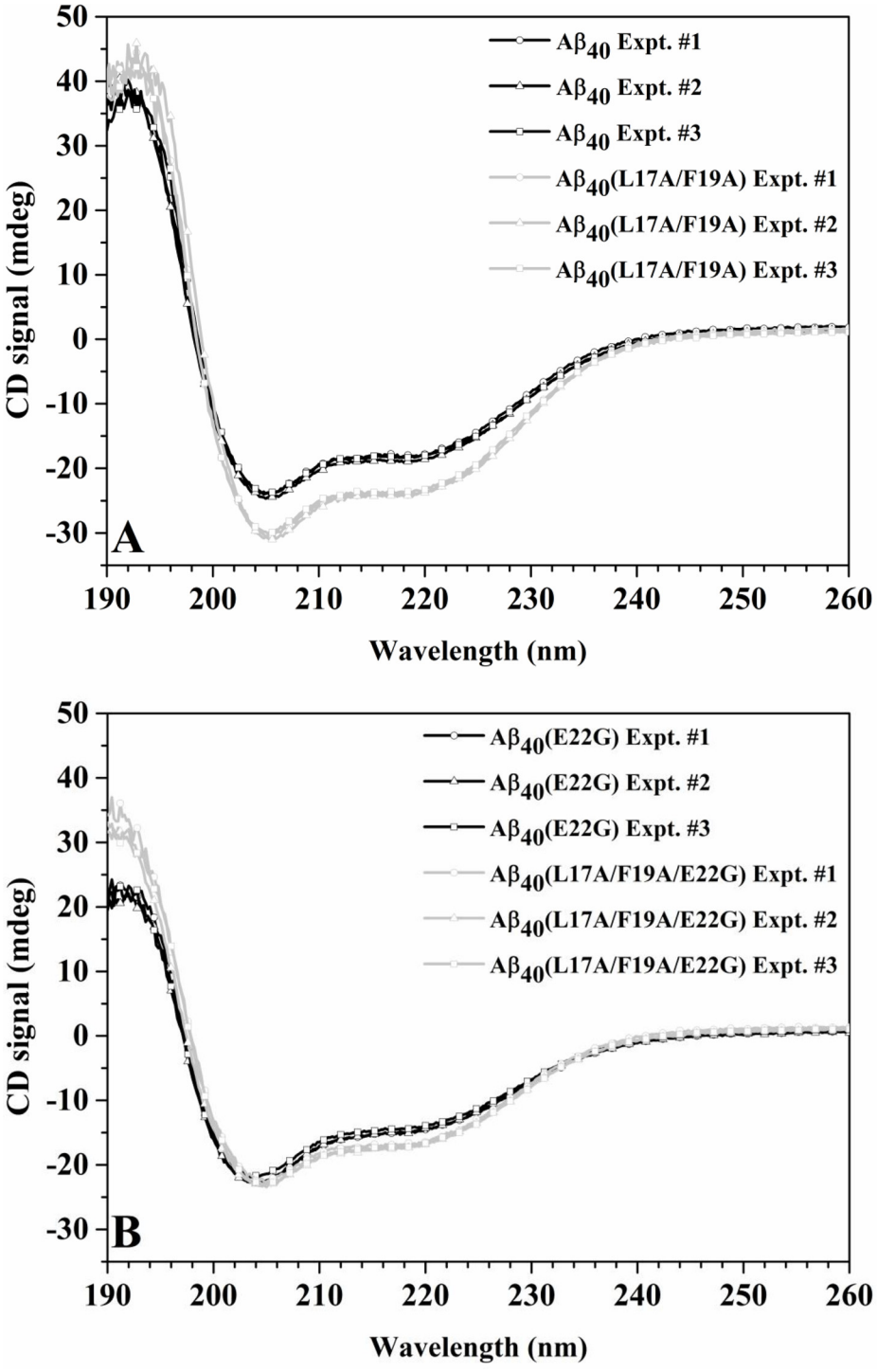

Fig 1. CD spectra of wild-type $A\beta_{40}$ and Arctic $A\beta_{40}$ variant in 100 mM SDS solution. (A) Superimposition of CD spectra of $A\beta_{40}$(L17A/F19A) (light grey) and wild-type $A\beta_{40}$ (black) in 100 mM SDS solution. (B) Superimposition of CD spectra of $A\beta_{40}$(L17A/F19A/E22G) (light grey) and $A\beta_{40}$(E22G) (black) in 100 mM SDS solution.

doi:10.1371/journal.pone.0154327.g001

Table 1. The secondary structure contents estimated from the CD spectra of Aβ peptides.

	$A\beta_{40}$	$A\beta_{40}$(L17A/F19A)	$A\beta_{40}$(E22G)	$A\beta_{40}$(L17A/F19A/E22G)
Helix	32.10 ± 0.26%	37.97 ± 0.91%	26.13 ± 0.35%	28.90 ± 0.26%
Antiparallel	13.47 ± 0.45%	9.03 ± 0.81%	24.10 ± 0.78%	18.50 ± 0.69%
Parallel	7.60 ± 0.10%	6.40 ±0.10%	8.70 ± 0.10%	8.13 ± 0.06%
Beta-turn	18.00 ± 0.10%	17.10 ± 0.17%	19.43 ± 0.12%	18.73 ± 0.06%
Random coil	26.13 ± 0.29%	21.67 ± 0.21%	28.63 ± 0.40%	27.37 ± 0.21%

The secondary structure contents were shown as the average **±** standard deviation from three individual CD experiments. Statistical analysis of the secondary structure contents was done by using GraphPad Prism Software (GraphPad Software, La Jolla, CA, USA). For helix, antiparallel and random coil values, the difference between $A\beta_{40}$ and $A\beta_{40}$(L17A/F19A) by one-way ANOVA analysis with a Tukey Multiple Comparison Test showed statistical significance ($p < 0.05$). There is no statistically significant difference for parallel and beta-turn values. The difference between $A\beta_{40}$(E22G) and $A\beta_{40}$(L17A/F19A/E22G) also show statistical significance for helix, antiparallel and random coil values, and no statistical significance for parallel and beta-turn values.

doi:10.1371/journal.pone.0154327.t001

were identified as S8, E11, H13-Q15, V18, F20-N27 (excluding L17 and F19), as compared to the previously assigned backbone resonances of $A\beta_{40}$(E22G) [14]. The backbone amide chemical shift differences between $A\beta_{40}$(E22G) and $A\beta_{40}$(L17A/F19A/E22G) were shown in Fig 3C. The majority of these residues that displayed noticeable chemical shift changes after L17A/F19A substitutions were also located within the α/β-discordant segment of $A\beta_{40}$(E22G). This effect induced by L17A/F19A substitutions was very similar to that observed in wild-type $A\beta_{40}$. Our NMR characterizations suggested that the increases of α-helicity observed by CD spectroscopy might mainly occur at the residues in the α/β-discordant segment of these double Ala-substituted peptides.

Since sequence effect may also induce chemical shift changes of amide proton and nitrogen cross-peaks, the chemical shift changes resulting from L17A/F19A substitutions might not solely come from the alteration of α-helical propensity. To verify whether the increases of α-helical propensities occurred at the residues in the α/β-discordant segment of these double Ala-substituted peptides, we further analyzed the $^{13}C^{\alpha}$ secondary chemical shifts of all mutant $A\beta_{40}$ peptides, and compared them with those of their native forms [14]. It has been reported that the $^{13}C^{\alpha}$ chemical shift is sensitive to protein backbone structure [17]. The $^{13}C^{\alpha}$ secondary chemical shift which is defined as the deviation of the observed $^{13}C^{\alpha}$ chemical shift of an amino acid residue from its $^{13}C^{\alpha}$ chemical shift in a random coil conformation has been used as a measure of secondary structure propensity [18]. For an amino acid residue in an α-helical conformation, it has an average $^{13}C^{\alpha}$ secondary chemical shift of 3.09 ± 1.0 ppm [17]. This value was used to estimate the percent α-helicity (% α-helicity) of an amino acid residue as well. Weinstock et al. showed that the percent α-helicity of an amino acid residue calculated from structure is quantitatively in agreement with that calculated from $^{13}C^{\alpha}$ secondary chemical shift, demonstrating that $^{13}C^{\alpha}$ secondary chemical shift is correlated to percent α-helicity [19]. The more positive $^{13}C^{\alpha}$ secondary chemical shifts represents the higher percent α-helicity. According to this correlation, we obtained that the replacements of L17 and F19 with alanines mainly augment the α-helicity of residues Q15, V18, F20 and E22-G25 (excluding L17 and F19) of wild-type $A\beta_{40}$ in SDS solution. Fig 4A showed that the $^{13}C^{\alpha}$ secondary chemical shifts of these residues were significantly more positive for $A\beta_{40}$(L17A/F19A) than for wild-type $A\beta_{40}$. The similar phenomenon was also observed in residues Q15-G25 of $A\beta_{40}$(L17A/F19A/E22G) and $A\beta_{40}$(E22G), as shown in Fig 4B, suggesting that residues Q15-G25 (excluding L17 and F19) of $A\beta_{40}$(L17A/F19A/E22G) adopted a higher α-helicity than those of $A\beta_{40}$(E22G).

Previously, Wishart et al. used chemical shit index (CSI) to determine secondary structure. An α-helix is identified as a group of three or more consecutive amino acid residues whose $^{13}C^{\alpha}$

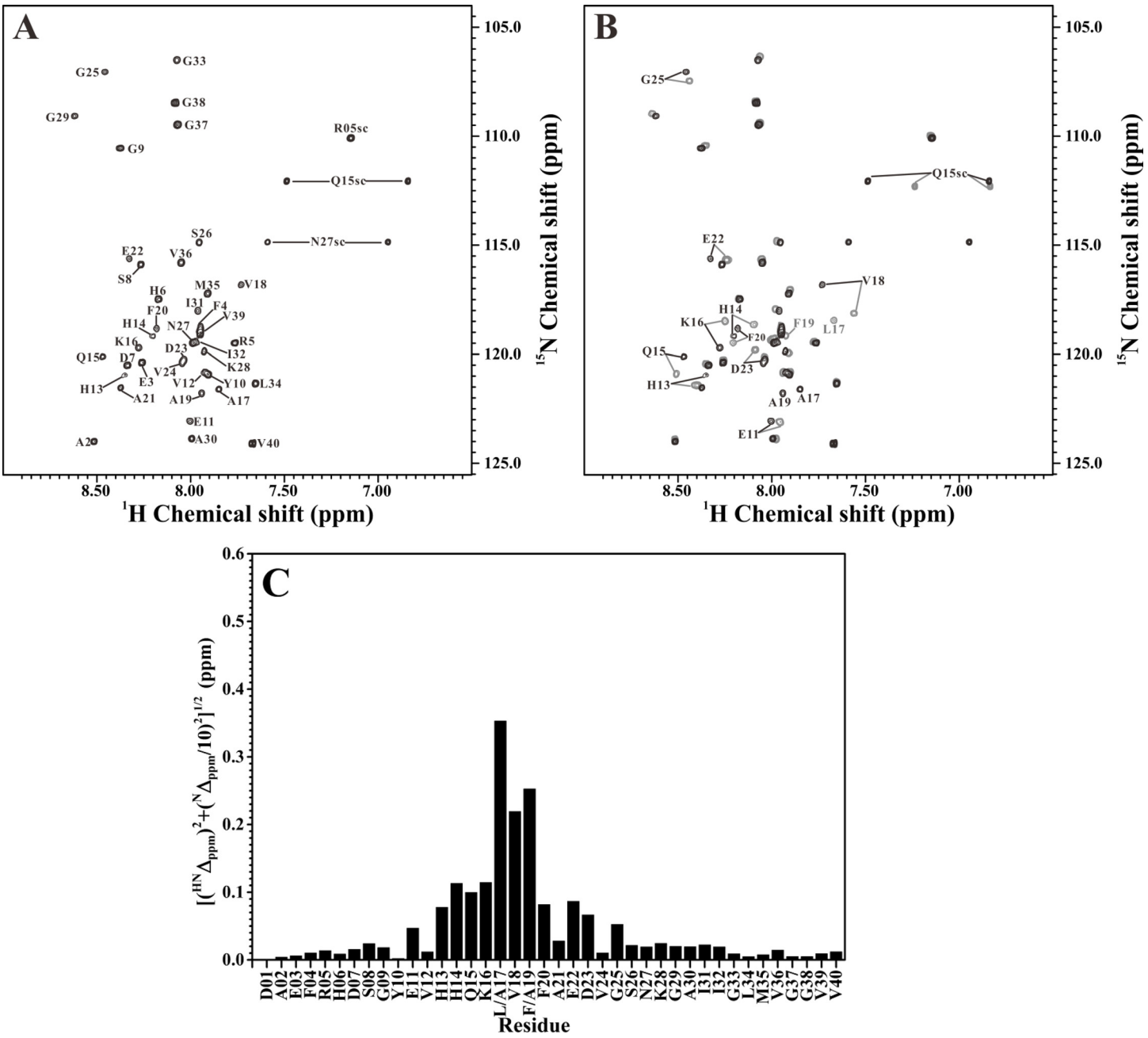

Fig 2. Comparison of the 2D ^{1}H-^{15}N-HSQC spectra of wild-type Aβ$_{40}$ and Aβ$_{40}$(L17A/F19A). (A) 2D ^{1}H-^{15}N-HSQC spectrum of Aβ$_{40}$(L17A/F19A) in 100 mM SDS solution. (B) Superimposition of 2D ^{1}H-^{15}N-HSQC spectra of Aβ$_{40}$(L17A/F19A) (black) and wild-type Aβ$_{40}$ (light grey) in 100 mM SDS solution. Residues with noticeable chemical shift changes were labeled. (C) The effect of L17A/F19A replacements on the backbone amide resonances of wild-type Aβ$_{40}$. The weighted chemical shift differences ($[(^{HN}\Delta_{ppm})^2+(^{N}\Delta_{ppm}/10)^2]^{1/2}$) were plotted as a function of residue number. $^{HN}\Delta_{ppm}$ and $^{N}\Delta_{ppm}$ were the $^{1}H^{N}$ and ^{15}N chemical shift differences between wild-type Aβ$_{40}$ and Aβ$_{40}$(L17A/F19A), respectively.

doi:10.1371/journal.pone.0154327.g002

secondary chemical shift were greater than 0.7 ppm [20]. It can be seen that the $^{13}C^{\alpha}$ secondary chemical shift of D23 in Aβ$_{40}$(E22G) was much less than 0.7 ppm, however, the $^{13}C^{\alpha}$ secondary chemical shift of D23 in Aβ$_{40}$(L17A/F19A/E22G) was greater than 0.7 ppm. This result suggested that the lost α-helicity at D23 of Arctic-type Aβ$_{40}$ [14] might be restored after L17A/F19A

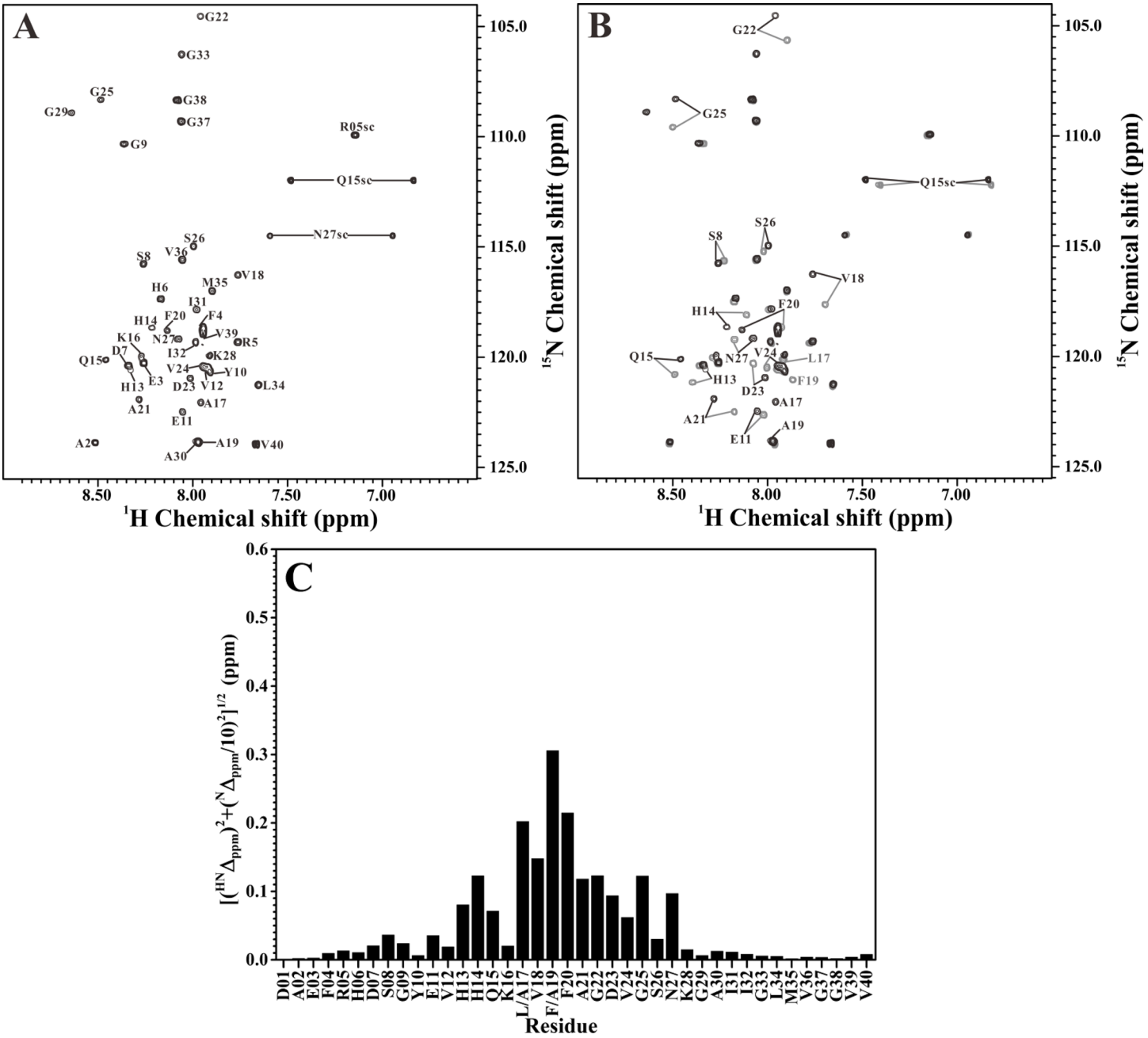

Fig 3. Comparison of the 2D ^{1}H-^{15}N-HSQC spectra of Aβ$_{40}$(E22G) and Aβ$_{40}$(L17A/F19A/E22G). (A) 2D ^{1}H-^{15}N-HSQC spectrum of Aβ$_{40}$(L17A/F19A/E22G) in 100 mM SDS solution. (B) Superimposition of 2D ^{1}H-^{15}N-HSQC spectra of Aβ$_{40}$(L17A/F19A/E22G) (black) and Aβ$_{40}$(E22G) (light grey) in 100 mM SDS solution. Residues with noticeable chemical shift changes were labeled. (C) The effect of L17A/F19A replacements on the backbone resonances of Aβ$_{40}$(E22G). The weighted chemical shift differences ($[(^{HN}\Delta_{ppm})^2+(^{N}\Delta_{ppm}/10)^2]^{1/2}$) were plotted as a function of residue number. $^{HN}\Delta_{ppm}$ and $^{N}\Delta_{ppm}$ were the $^{1}H^{N}$ and ^{15}N chemical shift differences between Aβ$_{40}$(E22G) and Aβ$_{40}$(L17A/F19A/E22G), respectively.

doi:10.1371/journal.pone.0154327.g003

substitutions. The results of $^{13}C^{\alpha}$ secondary chemical shift analysis further supported the fact that L17A/F19A substitutions mainly increased the α-helicity of the α/β-discordant segment in both wild-type and Arctic-type Aβ$_{40}$.

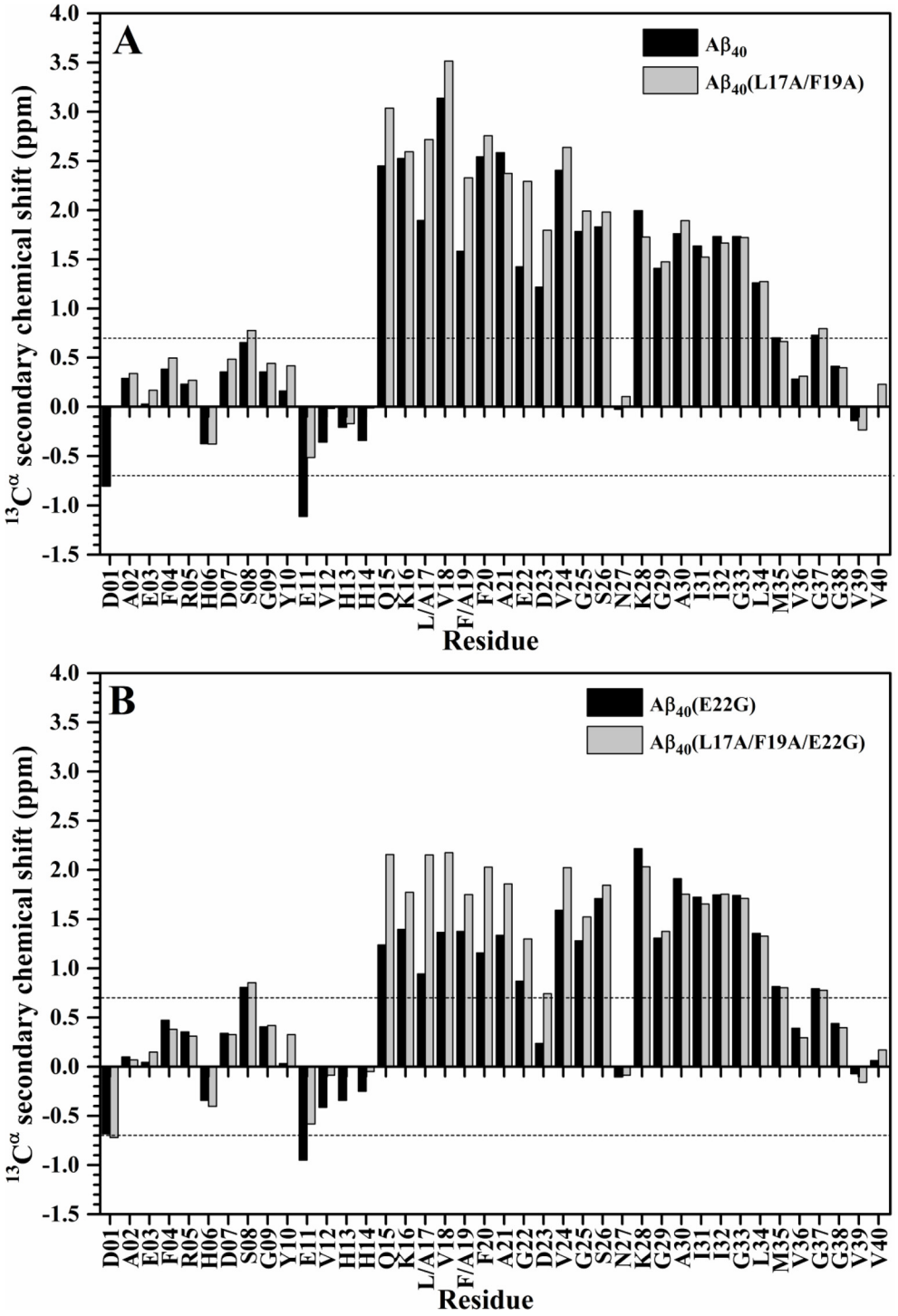

Fig 4. Comparison of $^{13}C^{\alpha}$ secondary chemical shifts of double Ala-substituted Aβ peptides and their native forms. (A) The plots of $^{13}C^{\alpha}$ secondary chemical shifts of $A\beta_{40}$(L17A/F19A) (light grey) and wild-type $A\beta_{40}$ (black) as a function of residue. (B) The plots of $^{13}C^{\alpha}$ secondary chemical shifts of $A\beta_{40}$(L17A/F19A/E22G) (light grey) and $A\beta_{40}$(E22G) (black) as a function of residue.

doi:10.1371/journal.pone.0154327.g004

Discussion

The structure of Aβ is dependent on the environments in which Aβ exists. It may adopt either random coil or α-helical conformation in different environments, such as in aqueous solution and SDS solution [21, 22]. The reason for using aqueous SDS solution to probe the α-helical propensity of Aβ and the relevance of this environment to biological systems have been discussed from a structural perspective in our previous publication [14]. In fibrillar form, Aβ mainly adopts β-strand conformation [23, 24]. The structure of nascent wild-type $A\beta_{40}$ residing in cellular membranes before unfolding remained unclear. However, the structure of C99, the transmembrane C-terminal domain of AβPP ($A\beta PP_{672\text{-}770}$), in lipid environments has been reported [25, 26]. The structure of wild-type $A\beta_{40}$ in SDS solution resembles the structure of the $A\beta_{40}$ domain ($A\beta PP_{672\text{-}711}$) in C99 in lipid environments and can be considered as the initial structure of wild-type $A\beta_{40}$ in cellular membranes. From a structural perspective, these suggested that Aβ peptides have to undergo a structural conversion from α-helix to β-strand during the aggregation process. From a thermodynamical point of view, the activation energy of structural conversion from α-helix to β-strand is closely related to the secondary structure propensity. For instance, a higher α-helical propensity would result in a higher activation energy for structural conversion from α-helix to β-strand. Thus, the secondary structure propensity of Aβ would be one key factor in governing its structural conversion tendency. Previously, Johannson and coworkers applied an *in silico* approach to predict amyloid fibril-forming proteins and proposed that these proteins contained an α/β-discordant sequence which is expected to form a β-strand but displays an α-helical structure in some environments and supposed to be prone to undergo a conformational transition from α-helix to β-strand. Aβ peptide was predicted to contain an α/β-discordant sequence located in the region of residues 16–23 [27], suggesting that the tendency for structural conversion of Aβ might be mainly governed by the secondary structure propensity of its α/β-discordant segment. It is likely that the structural transition occurred in the α/β-discordant segment prompted the aggregation cascade of Aβ peptide. Thus, any factor that varies the propensity of secondary structure in the α/β-discordant segment of Aβ would affect its structural conversion tendency, resulting in an alteration of Aβ aggregation propensity, such as mutation occurred in the α/β-discordant segment of Aβ. This conclusion has been confirmed by our recent studies [14]. We have demonstrated that Arctic mutation accelerates Aβ aggregation in SDS through diminishing the α-helicity of residues 15–25.

We previously found that the secondary structure of Aβ has relatively unstable residues, L17 and F19, in the α/β-discordant segment. L17A/F19A substitutions may reduce the rates of structural conversions and fibril formation of both wild-type [2] and Arctic-type $A\beta_{40}$ [3]. The result of *in silico* prediction also suggested that L17A/F19A substitutions may alter the propensity of the secondary structure of the α/β-discordant segment for both wild-type and Arctic-type $A\beta_{40}$. Fig 5 showed the secondary structures of the α/β-discordant segments obtained by using the propensity-based prediction [27]. In the present study, our data show that L17A/F19A substitutions can augment the α-helicity of the α/β-discordant segment for both peptides, confirming that an increase of the α-helical propensity of the α/β-discordant segment can stabilize the conformation and reduce the structural conversion tendency, in turn leading to a reduction of Aβ aggregation propensity.

A nucleation-dependent polymerization model has been pointed out to illustrate this complicated process for Aβ aggregated into amyloid fibril [28]. According to this model, the aggregation process of Aβ involves conformational changes and self-assembly. In addition to the intrinsic structural propensity of Aβ, the intramolecular and/or intermolecular interactions of Aβ also play an important role in the aggregation tendency of Aβ. In a real biological system,

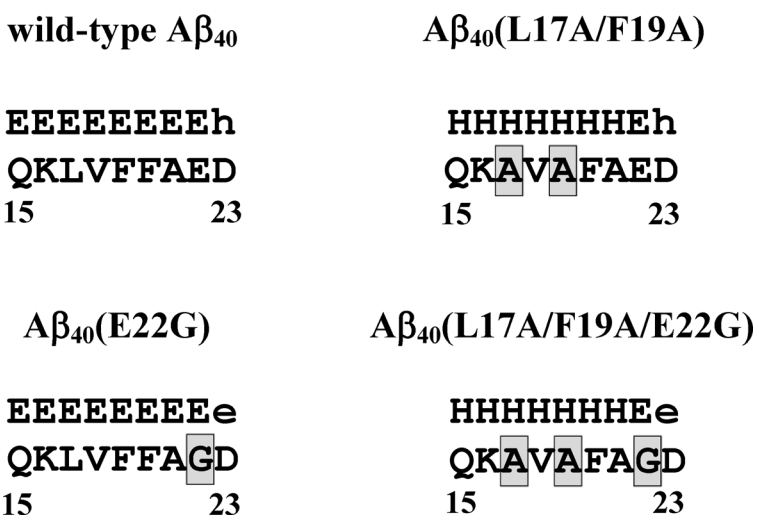

Fig 5. The predicted secondary structures of the α/β-discordant segments of double Ala-substituted Aβ peptides and their native forms. The secondary structure (upper row) for each amino acid residue was obtained by using the propensity-based prediction as described in Fig 2 caption of ref. 27. Adopting the notation used in Fig 2 caption of ref. 27, we denote the β-strands predicted with high and low probability by the symbols E and e, respectively. The symbols H and h were used for denoting the α-helical structures predicted with high and low probability, respectively.

doi:10.1371/journal.pone.0154327.g005

the interactions between Aβ and its local environments would affect its aggregation propensity. Moreover, the conformation of Aβ may influence these interactions as well. Mutation in the α/β-discordant segment of Aβ might alter not only the structural propensity but also these interactions. The effects of mutations on these two factors are profound. Either one factor could increase or reduce the structural conversion tendency of Aβ. The joint contribution of these two factors to the conformational conversion tendency of Aβ would result in a modulation of Aβ aggregation propensity. In the previous study [14], we found that Arctic mutation decreased the α-helical propensity of the α/β-discordant segment, leading to in an increase of the structural conversion tendency of Aβ. In this study, we obtain that L17/F19A substitutions exhibits an opposite effect on the structural propensity and structural conversion tendency of Aβ. These mutation studies provided the information about the role of the structural propensity of the α/β-discordant segment in Aβ aggregation propensity. However, the role of the interactions in Aβ aggregation propensity remains characterized. The α/β-discordant segment of Aβ covered residues 16–23. Besides the Arctic mutation, several FAD-linked AβPP mutations which promote α-helix-to-β-strand conversion and fibril formation [29, 30] were also located in this region. Whether other FAD-linked AβPP mutations have similar effects to Arctic mutation on the structural propensity of the α/β-discordant segment remains unknown. The effects of L17/F19A substitutions on the structural and aggregative propensities of other FAD-linked Aβ mutants need to be investigated. Study of the effect of these mutations on the structural and aggregative propensities of Aβ may help us gain more insight into the molecular mechanism of Aβ aggregation from a structural point of view.

Acknowledgments

The NMR spectra were obtained at the Core Facility for Protein Structural Analysis supported by National Core facility Program for Biotechnology, Instrumentation Center, National Taiwan University, and Taipei Veterans General Hospital.

Author Contributions

Conceived and designed the experiments: YCC THL. Performed the experiments: CTL HBH CCW YRC. Analyzed the data: CTL HBH YCC THL. Contributed reagents/materials/analysis tools: HBH CFC MSS YCC THL. Wrote the paper: CTL HBH YCC THL.

References

1. Wang CC, Huang HB, Tsay HJ, Shiao MS, Wu WJ, Cheng YC, et al. Characterization of Abeta aggregation mechanism probed by congo red. Journal of biomolecular structure & dynamics. 2012; 30 (2):160–9. Epub 2012/06/19. doi: 10.1080/07391102.2012.677767 PMID: 22702727.
2. Chen YR, Huang HB, Lo CJ, Wang CC, Su CL, Liu HT, et al. Abeta40(L17A/F19A) mutant diminishes the aggregation and neurotoxicity of Abeta40. Biochem Biophys Res Commun. 2011; 405(1):91–5. Epub 2011/01/11. doi: 10.1016/j.bbrc.2010.12.133 PMID: 21216230.
3. Chen YR, Huang HB, Lo CJ, Wang CC, Ho LK, Liu HT, et al. Effect of alanine replacement of l17 and f19 on the aggregation and neurotoxicity of arctic-type abeta40. PLoS One. 2013; 8(4):e61874. doi: 10.1371/journal.pone.0061874 PMID: 23634215; PubMed Central PMCID: PMC3636269.
4. Hilbich C, Kisters-Woike B, Reed J, Masters CL, Beyreuther K. Substitutions of hydrophobic amino acids reduce the amyloidogenicity of Alzheimer's disease beta A4 peptides. J Mol Biol. 1992; 228 (2):460–73. PMID: 1453457.
5. Esler WP, Stimson ER, Ghilardi JR, Lu YA, Felix AM, Vinters HV, et al. Point substitution in the central hydrophobic cluster of a human beta-amyloid congener disrupts peptide folding and abolishes plaque competence. Biochemistry. 1996; 35(44):13914–21. doi: 10.1021/bi961302+ PMID: 8909288.
6. Jana AK, Jose JC, Sengupta N. Critical roles of key domains in complete adsorption of Abeta peptide on single-walled carbon nanotubes: insights with point mutations and MD simulations. Physical chemistry chemical physics: PCCP. 2013; 15(3):837–44. doi: 10.1039/c2cp42933k PMID: 23203213.
7. Kumar J, Sim V. D-amino acid-based peptide inhibitors as early or preventative therapy in Alzheimer disease. Prion. 2014; 8(1):119–24. PMID: 24553069.
8. Carter MD, Simms GA, Weaver DF. The Development of New Therapeutics for Alzheimer's Disease. Clin Pharmacol Ther. 2010; 88(4):475–86. doi: 10.1038/clpt.2010.165 PMID: WOS:000282064000019.
9. Funke SA, Willbold D. Peptides for Therapy and Diagnosis of Alzheimer's Disease. Current pharmaceutical design. 2012; 18(6):755–67. PMID: WOS:000304416600003.
10. Findeis MA. Approaches to discovery and characterization of inhibitors of amyloid beta-peptide polymerization. Bba-Mol Basis Dis. 2000; 1502(1):76–84. doi: 10.1016/S0925-4439(00)00034-X PMID: WOS:000088710500008.
11. Kumar J, Namsechi R, Sim VL. Structure-Based Peptide Design to Modulate Amyloid Beta Aggregation and Reduce Cytotoxicity. PLoS One. 2015; 10(6):e0129087. doi: 10.1371/journal.pone.0129087 PMID: 26070139; PubMed Central PMCID: PMCPMC4466325.
12. Paivio A, Nordling E, Kallberg Y, Thyberg J, Johansson J. Stabilization of discordant helices in amyloid fibril-forming proteins. Protein Sci. 2004; 13(5):1251–9. Epub 2004/04/21. doi: 10.1110/ps.03442404 13/5/1251 [pii]. PMID: 15096631; PubMed Central PMCID: PMC2286751.
13. Lee EK, Hwang JH, Shin DY, Kim DI, Yoo YJ. Production of recombinant amyloid-beta peptide 42 as an ubiquitin extension. Protein expression and purification. 2005; 40(1):183–9. Epub 2005/02/22. doi: 10.1016/j.pep.2004.12.014 PMID: 15721787.
14. Lo CJ, Wang CC, Huang HB, Chang CF, Shiao MS, Chen YC, et al. The Arctic mutation accelerates Abeta aggregation in SDS through reducing the helical propensity of residues 15–25. Amyloid. 2015; 22(1):8–18. doi: 10.3109/13506129.2014.980943 PMID: 25376379.
15. Bohm G, Muhr R, Jaenicke R. Quantitative analysis of protein far UV circular dichroism spectra by neural networks. Protein Eng. 1992; 5(3):191–5. PMID: 1409538.
16. Greenfield NJ. Using circular dichroism spectra to estimate protein secondary structure. Nat Protoc. 2006; 1(6):2876–90. doi: 10.1038/nprot.2006.202 PMID: 17406547; PubMed Central PMCID: PMCPMC2728378.
17. Spera S, Bax A. Empirical Correlation between Protein Backbone Conformation and C-Alpha and C-Beta C-13 Nuclear-Magnetic-Resonance Chemical-Shifts. Journal of the American Chemical Society. 1991; 113(14):5490–2. doi: 10.1021/ja00014a071 WOS:A1991FU90000071.
18. Dyson HJ, Wright PE. Equilibrium NMR studies of unfolded and partially folded proteins. Nat Struct Biol. 1998; 5 Suppl:499–503. doi: 10.1038/739 PMID: 9665178.

19. Weinstock DS, Narayanan C, Baum J, Levy RM. Correlation between 13Calpha chemical shifts and helix content of peptide ensembles. Protein Sci. 2008; 17(5):950–4. Epub 2008/04/26. doi: 10.1110/ps.073365408 PMID: 18436960; PubMed Central PMCID: PMC2327285.

20. Wishart DS, Sykes BD. The 13C chemical-shift index: a simple method for the identification of protein secondary structure using 13C chemical-shift data. J Biomol NMR. 1994; 4(2):171–80. Epub 1994/03/01. PMID: 8019132.

21. Coles M, Bicknell W, Watson AA, Fairlie DP, Craik DJ. Solution structure of amyloid beta-peptide(1–40) in a water-micelle environment. Is the membrane-spanning domain where we think it is? Biochemistry. 1998; 37(31):11064–77. Epub 1998/08/07. doi: 10.1021/bi972979f [pii]. PMID: 9693002.

22. Hou L, Shao H, Zhang Y, Li H, Menon NK, Neuhaus EB, et al. Solution NMR studies of the A beta(1–40) and A beta(1–42) peptides establish that the Met35 oxidation state affects the mechanism of amyloid formation. J Am Chem Soc. 2004; 126(7):1992–2005. doi: 10.1021/ja036813f PMID: 14971932.

23. Petkova AT, Ishii Y, Balbach JJ, Antzutkin ON, Leapman RD, Delaglio F, et al. A structural model for Alzheimer's beta -amyloid fibrils based on experimental constraints from solid state NMR. Proc Natl Acad Sci U S A. 2002; 99(26):16742–7. doi: 10.1073/pnas.262663499 PMID: 12481027; PubMed Central PMCID: PMC139214.

24. Parthasarathy S, Inoue M, Xiao Y, Matsumura Y, Nabeshima Y, Hoshi M, et al. Structural Insight into an Alzheimer's Brain-Derived Spherical Assembly of Amyloid beta by Solid-State NMR. J Am Chem Soc. 2015; 137(20):6480–3. doi: 10.1021/jacs.5b03373 PMID: 25938164; PubMed Central PMCID: PMCPMC4462565.

25. Barrett PJ, Song Y, Van Horn WD, Hustedt EJ, Schafer JM, Hadziselimovic A, et al. The amyloid precursor protein has a flexible transmembrane domain and binds cholesterol. Science. 2012; 336(6085):1168–71. doi: 10.1126/science.1219988 PMID: 22654059; PubMed Central PMCID: PMC3528355.

26. Song Y, Mittendorf KF, Lu Z, Sanders CR. Impact of bilayer lipid composition on the structure and topology of the transmembrane amyloid precursor C99 protein. J Am Chem Soc. 2014; 136(11):4093–6. doi: 10.1021/ja4114374 PMID: 24564538; PubMed Central PMCID: PMC3985881.

27. Kallberg Y, Gustafsson M, Persson B, Thyberg J, Johansson J. Prediction of amyloid fibril-forming proteins. J Biol Chem. 2001; 276(16):12945–50. Epub 2001/01/13. doi: 10.1074/jbc.M010402200 PMID: 11134035.

28. Lomakin A, Teplow DB, Kirschner DA, Benedek GB. Kinetic theory of fibrillogenesis of amyloid beta-protein. Proc Natl Acad Sci U S A. 1997; 94(15):7942–7. Epub 1997/07/22. PMID: 9223292; PubMed Central PMCID: PMC21534.

29. Murakami K, Irie K, Morimoto A, Ohigashi H, Shindo M, Nagao M, et al. Synthesis, aggregation, neurotoxicity, and secondary structure of various A beta 1–42 mutants of familial Alzheimer's disease at positions 21–23. Biochem Biophys Res Commun. 2002; 294(1):5–10. Epub 2002/06/11. doi: 10.1016/S0006-291X(02)00430-8 [pii]. PMID: 12054732.

30. Morimoto A, Irie K, Murakami K, Ohigashi H, Shindo M, Nagao M, et al. Aggregation and neurotoxicity of mutant amyloid beta (A beta) peptides with proline replacement: importance of turn formation at positions 22 and 23. Biochem Biophys Res Commun. 2002; 295(2):306–11. Epub 2002/08/02. doi S0006291X02006708 [pii]. PMID: 12150948.